Local-field enhancement on rough surfaces of metals, semimetals, and semiconductors with the use of optical second-harmonic generation

G. T. Boyd, Th. Rasing, J. R. R. Leite,* and Y. R. Shen
Department of Physics, University of California, Berkeley, California 94720
and Materials and Molecular Research Division, Lawrence Berkeley Laboratory, Berkeley, California 94720
(Received 21 February 1984)

Optical second-harmonic generation was used to study the local-field enhancement due to surface roughness on various materials ranging from the alkalis to a semiconductor. The roughness morphology was standardized by evaporating each material onto the same chemically etched glass slide, having microstructures hundreds to thousands of angstroms in size. With the laser excitation at 1.06 μm, the observed second-harmonic enhancements for different materials varied from 27 to 1×10^{-3} times that of silver. They were in fair agreement with a simple model calculation assuming that the rough surface is composed of a distribution of noninteracting hemispheroids on a plane. The results are used to predict some rather substantial enhancements for surface Raman scattering for a number of substrate materials.

I. INTRODUCTION

The effective Raman cross section of molecules can increase by many orders of magnitude when adsorbed on roughened noble-metal surfaces.[1] The cause of this surface-enhanced Raman scattering (SERS) effect, and its promise as a new and sensitive tool for surface spectroscopy, continue to attract considerable attention. It is generally accepted that there are two distinct contributions to the enhancement. First, a chemical interaction between the adsorbed molecules and the substrate can lead to an intrinsic Raman cross section that is different from that of the isolated molecules. Second, the incoming and outgoing optical fields can be enhanced because of local-field enhancement resulting from local-plasmon resonances and corona (or lightning-rod) effects in the rough surface protrusions. For noble metals, the second mechanism is believed to be dominant.[1]

One expects, from the local-field enhancement alone, that any roughened conductor could produce surface-enhanced Raman scattering, although the magnitude of enhancement may vary. However, very few materials have actually been examined.[1–17] Measuring the relative enhancement ability of various metals using Raman scattering is complicated by the fact that in many cases even the SERS signal is too weak to detect, and that the surface coverage of adsorbates on different substrates varies widely and is very difficult to determine. If we are only interested in the local-field enhancement, then it is actually more appropriate to study the surface enhancement of some other optical effects which occur on bare substrates and require no adsorbates. Optical mixing on surfaces is an example. It should occur at a surface with or without adsorbates. Second-harmonic generation (SHG) is particularly attractive because the experimental arrangement is simple and it provides easily detectable signals from both smooth and rough metal surfaces. In addition, SHG and Raman scattering have essentially identical dependences on the local-field enhancement at the surface.[18] Four-wave mixing and higher-order processes generate hardly detectable signals from smooth surfaces. They are generally not useful as means to study surface enhancement.

Because SHG from both smooth and rough surfaces of any material is easily detectable, we can use it to measure the local-field enhancement at the surface of a variety of substances. In this paper we report our measurements on 16 different metals and one semiconductor. The surface local-field enhancement is defined as the ratio of the second-harmonic (SH) intensity from the rough surface to that from the smooth surface. Identical roughness was established for each material by evaporating the materials onto the same glass slide which had been roughened. Using this method, we could derive the relative surface enhancement of different materials, and find that several materials should have sufficiently high surface enhancement to be useful in surface Raman spectroscopy and other surface optical studies.

Our results also provide a quantitative test for the surface local-field theory[18] The local-field enhancement is expected to depend critically on the dielectric constant of the material. The wide range of materials with a wide range of dielectric constants used in our study can, therefore, subject the theory to a stringent test. The predictions were found to be in good agreement with our measurements. We can then use the theory to predict the local-field enhancement in surface Raman scattering for various materials.

In addition, the SH measurements from smooth surfaces of various materials allowed us to estimate the second-order nonlinear-optical coefficients for these materials. For many metals, they appeared to be within an order of magnitude of the predictions from a simple free-electron model.

II. EXPERIMENT AND RESULTS

The rough and smooth surfaces were prepared by evaporating films of each material simultaneously onto

smooth and roughened glass slides. The roughened slide had random, irregular surface protrusions, hundreds to thousands of angstroms in size, produced by chemically etching a single face of a microscope slide with hydrofluoric acid vapor. The slide was precleaned with soap and water, masked on one side, and then heated to approximately 100 °C. It was then immersed into a sealed enclosure of warm (30 °C) HF vapor, removed after about 10 min, then rinsed thoroughly with distilled water. The heating was necessary to prevent large HF droplets from condensing onto the glass and dissolving the vapor-etched fine structures. Silver evaporated onto the etched slide gave somewhat less, but comparable, SH enhancements, and showed similar surface features to that of electrolytically reformed silver, which is widely used to obtain large SERS enhancements.

The roughened slide was reused after each measurement by dissolving the evaporated film in aqua regia, and then cleaning the slide in distilled water and drying it with nitrogen gas. A fresh, smooth slide was used in each measurement and cleaned in a similar way. Since both the rough and smooth surfaces were subject to the same cleaning conditions, their intrinsic optical coefficients for SH generation were presumed to be the same. The measurements were fairly reproducible. It then suggested that the ratio of the SH intensities from roughened and smooth surfaces should be nearly independent of possible surface contamination.

The repeated cleaning and evaporation procedure did not significantly alter the etched surface. The SH intensity from the roughened surface of all the materials was reproducible to within a factor of 2 or better, after many cleanings and evaporations. The SH intensity from the smooth surfaces was reproducible to within 20%. Such variations were "felt" to be acceptable, compared to the many orders of magnitude over which the measured SH enhancements ranged.

The materials in this study had a wide range of dielectric constants: good conductors such as the alkali and noble metals, moderate conductors such as tin, lead, and nickel, as well as the semimetal bismuth and the semiconductor germanium. All materials were at least 99.9% pure.

The SH signals were obtained from the glass-tin interfaces. High evaporation rates, typically 100 Å/sec, and low pressures, $<10^{-6}$ Torr, in the evaporation chamber were used to ensure the purity of the interface. Protection from oxidation for those measurements made in air was provided by evaporating films at least 3000 Å thick. The alkali-metal films were kept under vacuum during the measurement in a specially constructed evaporation chamber equipped with a liquid-nitrogen vapor trap. During the course of each measurement, the SH intensity from the samples never varied by more than 20%, and the smooth surfaces always maintained their shininess.

The apparatus for measuring the SH enhancement is shown in Fig. 1. A Q-switched neodium:yttrium-aluminum-garnet (Nd:YAG) laser provided 6-nsec excitation pulses at 1.06 μm. The p-polarized beam, incident at 45° to the samples, was spectrally filtered to exclude any SH radiation generated before the sample. Input intensities at the samples were on the order of 1 MW/cm^2 with a beam diameter of 0.5 cm. The SH signals reflected from the glass-film interface were spectrally filtered to block the fundamental excitation. The signals were then collected by a $f/2$ lens, sent through an angularly tuned interference filter, and finally focused onto a photomultiplier tube (PMT). An additional spectral filter at the PMT served to clock stray 1.06-μm light. Large SH signals were attenuated by calibrated neutral-density filters. The electrical pulses from the PMT were processed by a gated integrator and averaged by a microcomputer over 800 laser shots. Standard deviations from the mean were less than 10% of the averages, primarily due to laser-pulse fluctuations and photon-counting statistics.

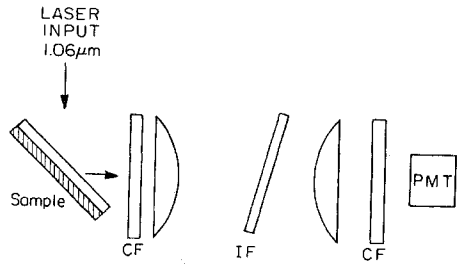

FIG. 1. Experimental setup. CF, spectral filter; IF, interference filter; PMT, photomultiplier tube.

The SH radiation from the rough surfaces was diffused and unpolarized. The $f/2$ lens served to collect approximately 10% of the diffuse light. The smooth surfaces provided a collimated and p-polarized SH signal which was focused by the collection lens. An iris was placed at the focal point to pass the collimated light and block any diffuse light. Tests with spectral filters confirmed that the SH signals originated from the samples.

A simple experiment by Chen *et al.*[19] on electrolytically roughened noble-metal surfaces in air revealed significant broadband luminescence near the SH peak. We measured the signal spectrum near the SH for all the samples using an angle-tuned interference filter [40 Å full width at half maximum (FWHM)]. Luminescence at 0.532 μm was then estimated and subtracted from the measured SH signal to obtain the true SH signal. We found that for our samples, the luminescence was comparable to the SH signal from the roughened surfaces of only a few materials: Mn, Fe, Ni, and Ge. The ratio of the luminescence to the SH from copper and gold samples was much less than that reported by Chen *et al.*[19] It is possible that their luminescence background resulted from remnants of the electrolytic roughening process.

The SH signals from the smooth surfaces of each material were ratioed to that from gold. This comparison served to normalize all measurements against variations in the incident-beam characteristics. The measured SH enhancements from rough surfaces of different materials were then ratioed to that of silver. Both the normalized SH surface enhancements and the normalized SH signals from different materials are listed in Table I. The absolute value of the SH enhancement for silver evaporated onto our roughened slide was 2.0×10^3. It is seen that

TABLE I. SH data.

Material	SH enhancement relative to $_{47}$Ag	SH intensity from smooth films relative to $_{47}$Ag
$_{31}$Ga	27	1.0×10^{-2}
$_{13}$Al	4.6	1.7×10^{-2}
$_{12}$Mg	7.0×10^{-1}	5.9×10^{-1}
$_{11}$Na	3.6×10^{-1}	13
$_{19}$K	6.0×10^{-2}	67
$_{37}$Rb	4.0×10^{-2}	69
$_{82}$Pb	2.6×10^{-2}	3.5×10^{-2}
$_{28}$Ni	1.2×10^{-2}	8.8×10^{-3}
$_{50}$Sn	1.1×10^{-2}	1.1×10^{-1}
$_{29}$Cu	1.0×10^{-2}	1.6
$_{83}$Bi	9.2×10^{-3}	2.1×10^{-1}
$_{79}$Au	8.3×10^{-3}	5.4
$_{32}$Ge	4.4×10^{-3}	1.1×10^{-2}
$_{49}$In	4.0×10^{-3}	3.8×10^{-1}
$_{26}$Fe	1.6×10^{-3}	6.1×10^{-2}
$_{25}$Mn	4.2×10^{-4}	3.0×10^{-2}

several good conductors display local-field enhancements comparable to or larger than that of silver, while poorly conducting metals, semimetals, and semiconductor Ge have much weaker enhancements. Overall, the enhancements range over 4 orders of magnitude. Since SH generation has essentially the same local-field dependence as Raman scattering (see Sec. III), the results in Table I give an immediate estimate of the local-field enhancements for SERS on the same materials. A more detailed discussion of these results will follow the next section.

III. THEORY AND COMPARISON WITH EXPERIMENT

The enhancement of optical signals from adsorbates on roughened surfaces is due to both chemical and electromagnetic interactions.[18,20,21] By chemical interactions, we mean the significant modification on the eigenenergies and eigenfunctions of a molecule in the absence of any applied field, when adsorbed onto a substrate. With the presence of an applied field, induced-dipole—induced-dipole interaction between molecules and induced-dipole—image-dipole interaction between the molecules and substrate also occur. This we refer to as the microscopic local-field effect.[22] A second type of electromagnetic effect is the change in the incoming and outgoing fields at the surface of a substrate according to the macroscopic Maxwell equations and the surface-boundary conditions. This is the macroscopic local-field effect which can lead to another local-field enhancement. On a bare substrate surface without adsorbates, the enhancement of optical signals from the rough surface can only come from the electromagnetic interaction. The microscopic local field is expected to be the same for smooth and rough surfaces. Therefore, the surface enhancement should be the result of only the macroscopic local-field enhancement.

The macroscopic local-field enhancement can be very large on rough surfaces which have protrusions on the order of hundreds to thousands of angstroms. Fields tend to concentrate at the tips of these protrusions in an effort to be nearly perpendicular to a metal or semiconductor surface. This is known as the lightning-rod effect.[23,24] In addition, collective oscillation of the electrons in these protrusions can be induced by the optical fields. The resonance produces a large local-field enhancement, which is referred to as the local-plasmon effect.[23,24] These are the dominant field-enhancement mechanisms at rough surfaces.

Chen *et al.*[18] have used the local-field correction factor to describe the macroscopic local-field enhancement. For the rough surface, the following simple model was assumed: The surface is represented by a collection of noninteracting hemispheriods sitting upward on a plane (Fig. 2). In the presence of an infinite plane wave $\vec{E}(\omega)$, the local fields just outside and inside a hemispheriod are, respectively,[23,25]

$$\vec{E}_L^{\,\mathrm{out}}(\omega)=[L_{||}^{\mathrm{out}}(\omega)\sin\alpha\,\hat{\eta}+L_{\perp}^{\mathrm{out}}(\omega)\cos\alpha\,\hat{\xi}]E_{\perp}(\omega)\ ,$$
$$\vec{E}_L^{\,\mathrm{in}}(\omega)=[L_{||}^{\mathrm{in}}(\omega)\sin\alpha\,\hat{\eta}+L_{\perp}^{\mathrm{in}}(\omega)\cos\alpha\,\hat{\xi}]E_{\perp}(\omega)\ , \tag{1}$$

where $E_{\perp}(\omega)$ is the plane-wave component perpendicular to the plane, and the angle α and unit vectors $\hat{\eta}$ and $\hat{\xi}$ are defined in Fig. 2. The local-field correction factor L satisfies the relations

$$L_{||}^{\mathrm{in}}(\omega)=L_{\perp}^{\mathrm{in}}(\omega)=L_{||}^{\mathrm{out}}(\omega)=\frac{\epsilon(\omega)}{\epsilon_m(\omega)}L_{\perp}^{\mathrm{out}}(\omega)\ ,$$
$$L_{||}^{\mathrm{out}}(\omega)=L_{\mathrm{LR}}L_p(\omega)\ , \tag{2}$$

with

$$L_{\mathrm{LR}}=1/A\ ,$$
$$L_p=\frac{\epsilon_m}{\epsilon}\Big/\left[\epsilon_m/\epsilon-1+(1/A)\left[1+i\frac{4\pi^2V}{3\lambda^3}(1-\epsilon_m)\epsilon^{1/2}\right]\right]\ ,$$

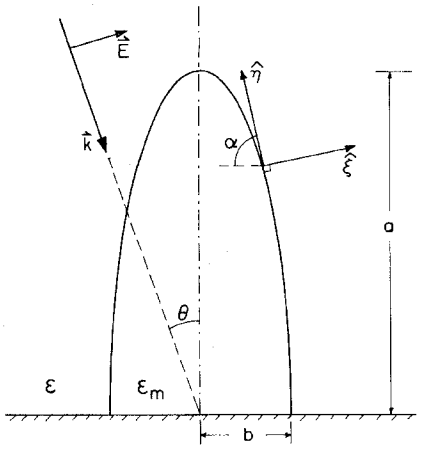

FIG. 2. Rough surface model.

where $A=[1-\xi Q_1'(\xi)/Q_1(\xi)]^{-1}$, $\xi=[1-(b/a)^2]^{-1/2}$ and $Q_1(\xi)=(\xi/2)\ln[(\xi+1)/(\xi-1)]^{-1}$ is the Legendre function of the second kind,[26] $Q_1'=dQ_1/d\xi$, ϵ_m, and ϵ are the dielectric constants of the hemispheriod and the surrounding medium, respectively, $V=\frac{4}{3}\pi ab^2$ is the full spheroid volume, and λ is the wavelength of the driving field. We shall use this model to discuss the surface enhancement of SHG from various materials.

The lightning-rod and local-plasmon-resonance contributions to the local field are explicitly exhibited in the factors $L_{\rm LR}$ and L_p, respectively. $L_{\rm LR}$ is a function only of the hemispheroid shape, given by the aspect ratio a/b. For a hemisphere, $a/b=1$, we have $L_{\rm LR}=3$. For elongated hemispheroids, $a/b\gg1$, we have $L_{\rm LR}\simeq(a/b)^2/\ln(a/b)\gg1$. A plot of $L_{\rm LR}$ versus a/b is given in Fig. 3(a).

The local-plasmon factor L_p may also be much larger than unity. Its resonance occurs when the frequency $\omega=\omega_0$ satisfies the relation

$$\mathrm{Re}\frac{\epsilon_m(\omega_0)}{\epsilon(\omega_0)}=1-1/A(a/b)\ . \tag{3}$$

We have, on resonance,

$$|L_p(\omega_0)|=\frac{\epsilon_m(\omega_0)}{\epsilon(\omega_0)}\Big/\left[\mathrm{Im}\left[\frac{\epsilon_m(\omega_0)}{\epsilon(\omega_0)}\right]+\frac{1}{A(a/b)}\frac{4\pi^3}{3}\frac{V}{\lambda_0^3}[1-\epsilon_m(\omega_0)][\epsilon(\omega_0)]^{1/2}\right]\ . \tag{4}$$

The resonant enhancement is limited by the damping factors in the denominator. The first term, $\mathrm{Im}(\epsilon_m/\epsilon)$, is determined by the characteristic loss in the hemispheroid. If l is the mean free path of electrons in the bulk and b is the smaller hemispheroid dimension, then $\mathrm{Im}(\epsilon_m)$ is that of the bulk multiplied by $1+l/b$, often known as the wall-collisional effect.[27] The other damping term in Eq. (3) is caused by radiation loss.[27] The field, enhanced by $L_{\rm LR}=1/A(a/b)$, induces a dipole moment in the hemispheroid which radiates with a dipolelike $1/\lambda^3$ dependence and a power proportional to the number of oscillating electrons. In a free-electron metal, the number of electrons is proportional to $[1-\epsilon_m(\omega)]V$. Expanding the hemispheroid volume increases the radiative damping, but decreases the wall-collisional damping. Therefore, an optimum value of V exists.

The local-field correction factor $L_\perp^{\rm out}=L_{\rm LR}L_p$ is plotted against a/b in Fig. 3(b) for a metal hemispheroid with an electron density $N_e=10^{23}$ cm^{-3} and a bulk mean free path of 500 Å, close to that of silver. The wavelength is fixed at $\lambda=1.06$ μm. The dashed curve shows the sharp plasmon resonance when only the bulk $\mathrm{Im}(\epsilon_m)$ damping is considered. A near-optimum value of $V=5\times10^{-4}\lambda^3$ was chosen to include the wall-collisional–damping contribution in curve (2) and the additional radiative damping contribution in curve (3). The resonant peak is shifted to a smaller value of a/b for curve (4) when N_e is reduced to 10^{22} cm^{-3}, since from Eq. (3), we have $\mathrm{Re}(\epsilon_m/\epsilon)\simeq-\omega_p^2/\omega_0^2=A$, which decreases with a/b. The value of $|L_\perp^{\rm out}|$ also decreases with a/b because of the smaller lightning-rod factor $L_{\rm LR}$.

The above discussion is for a single hemispheroid. The rough surfaces used in surface-enhancement experiments actually contain protrusions of a wide variety of shapes and sizes. Our model then assumes that the rough surface can be approximated by a set of noninteracting hemispheroids of randomly distributed sizes and shapes, that is, a random distribution of a and b values. In this model, any optical frequency can find some resonant protrusions on the surface. According to the local-plasmon-resonance condition of Eq. (3), lower frequencies should find plasmon resonances in the more elongated protrusions, which will yield a large lightning-rod effect. Thus, the local-field enhancement for the rough metal surface should increase monotonically with the wavelength. At a given frequency, ω, a range of different protrusions can be near resonance. A broader resonant peak in the plot of L versus a/b in Fig. 3(b) indicates that more near-resonant protrusions contribute to the local-field enhancement. Although increased damping reduces the amplitude of the plasmon resonance, the additional broadening, on the contrary, can help the enhancement.

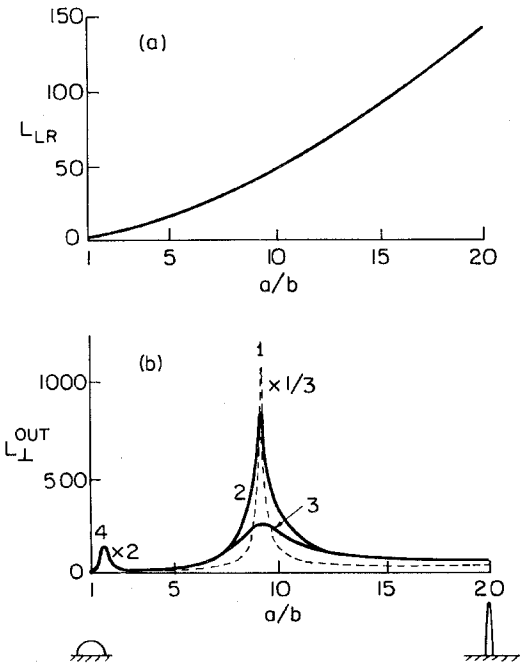

FIG. 3. Plot versus a/b of (a) the lightning-rod factor $L_{\rm LR}$ and (b) the local-field factor $L_\perp^{\rm out}$ with (1) bulk $\mathrm{Im}(\epsilon_m)$ damping only, (2) wall-collisional damping included, and (3) further addition of radiative damping. Curve (4) is for a metal with a lower electron density, including all damping effects.

The local-field correction factors can be used to calculate the enhancement of an optical signal from a rough surface. In the calculation, we clearly need to sum over the random distribution of the hemispheroidal shapes and sizes.

We now consider the local-field enhancement of SHG from a rough surface relative to that from a smooth surface. For p-polarized excitation, the SH power from a smooth surface, characterized by a second-order polarizability $\vec{\vec{\alpha}}^{(2)}$, is given by[18]

$$P_{\mathrm{SH}}(2\omega)=\frac{2\pi c}{\sqrt{\epsilon}}\left[\frac{2\omega}{c}\right]^2 N^2\mathscr{A}\,|\,\hat{n}\times\vec{\vec{\alpha}}^{(2)}\vdots\vec{\vec{\mathrm{L}}}(2\omega)\vec{\vec{\mathrm{L}}}(\omega)\vec{\vec{\mathrm{L}}}(\omega)\vec{\mathrm{E}}(\omega)\vec{\mathrm{E}}(\omega)\,|^2_{\mathrm{plane}}\sec\theta\ , \tag{5}$$

where the input at ω is incident on the plane at an angle θ and illumines an area $\mathscr{A}$ containing N atoms per unit area. The output at 2ω progagates in the direction $\hat{n}$. The local-field tensor $\vec{\vec{\mathrm{L}}}$ for the plane follows directly from the Fresnel equations. Just inside the substrate, we find

$$L_{\perp}^{\mathrm{in}}=(\epsilon/\epsilon_m)(1+r)\ ,\quad L_{\parallel}^{\mathrm{in}}=1-r\ , \tag{6}$$

in which r is the reflection coefficient of a p-polarized field.

We shall assume that $\alpha^{(2)}_{\parallel\perp\parallel}$ dominates in $\vec{\vec{\alpha}}^{(2)}$ for simplicity, as suggested in Ref. 18. The SH output from the smooth surface then becomes

$$P_{\mathrm{plane}}(2\omega)=\frac{8\pi c}{\sqrt{\epsilon}}\left[\frac{2\omega}{c}\right]^2 N^2\mathscr{A}\,|\,\alpha^{(2)}_{\parallel\perp\parallel}L_{\parallel}^{\mathrm{in}}(2\omega)L_{\perp}^{\mathrm{in}}(\omega)L_{\parallel}^{\mathrm{in}}(\omega)\,|^2_{\mathrm{plane}}E^4(\omega)\cos^3\theta\sin^2\theta\ . \tag{7}$$

The SH power from a highly elongated hemispheroid, $a/b\gg 1$, has been calculated by Chen *et al.*[18] A modification of their result yields

$$P_{\mathrm{hemisph}}(2\omega)=\frac{2^7}{3}\pi^2 c\sqrt{\epsilon}\left[\frac{2\omega}{c}\right]^4 N^2b^4x^2\,|\,\alpha^{(2)}_{\parallel\perp\parallel}L_{\parallel}^{\mathrm{in}}(2\omega)L_{\perp}^{\mathrm{in}}(\omega)L_{\parallel}^{\mathrm{in}}(\omega)\,|^2_{\mathrm{hemisph}}E^4(\omega)\sin^4\theta\ , \tag{8}$$

where

$$x(a/b)=\{(a/b)^2/[(a/b)^2-1)]\}\{1-[\ln(a/b)^2]/[(a/b)^2-1]\}$$

is a geometric function which generalizes the result of Chen *et al.* to include all hemispheroids with aspect ratio $a/b>1$. The ratio of $P_{\mathrm{hemisph}}(2\omega)$ to $P_{\mathrm{plane}}(2\omega)$ with $\mathscr{A}=\pi b^2$ yields the enhancement factor

$$\eta_{\mathrm{SH}}(a/b)=\frac{4\pi}{3}\left[\frac{\pi(bx)^2}{\lambda^2}\right]\sin^2\theta\sec^3\theta 2^6\frac{|\,L_{\parallel}^{\mathrm{in}}(2\omega)L_{\perp}^{\mathrm{in}}(\omega)L_{\parallel}^{\mathrm{in}}(\omega)\,|^2_{\mathrm{hemisph}}}{|\,L_{\parallel}^{\mathrm{in}}(2\omega)L_{\perp}^{\mathrm{in}}(\omega)L_{\parallel}^{\mathrm{in}}(\omega)\,|^2_{\mathrm{plane}}}\ , \tag{9}$$

which is primarily dependent on the ratio of the local-field correction factors for the hemispheroid and plane. The factor of 2^6 comes from the image of the hemispheroid fields in the conducting plane. The factor in large parentheses is a ratio of the area of the hemispheroid and plane which radiate the fundamental fields in phase to generate the SH.

We finally sum the contributions from hemispheroids of various shapes and sizes, assuming equal probability distribution with reasonable cutoff points, to obtain the total SH enhancement:

$$\eta^T_{\mathrm{SH}}=C[\Delta(a/b),\Delta V]\sum_{V,a/b}\eta_{\mathrm{SH}}(a,b)\ , \tag{10}$$

where $C[\Delta(a/b),\Delta V]$ is the fraction of the illuminated area occupied by hemispheroids with volume $V=\frac{4}{3}\pi ab^2\pm\Delta V$ and aspect ratio $a/b\pm\Delta(a,b)$.

The local-field enhancement of Raman scattering can be similarly calculated.[18] It is usually defined as the ratio of the Raman signal from molecules adsorbed uniformly on a rough surface to that of the same number of molecules in space. Assuming that the $\alpha^R_{\perp\perp}$ component of the Raman polarizability tensor dominates, we find the total surface enhancement as

$$\eta^T_R=C[\Delta(a/b),\Delta V]\sum_{V,a/b}\eta_R(a,b)\ , \tag{11}$$

where

$$\eta_R(a,b)=\frac{2}{\pi}\sin^2\theta(b/a)^3\sqrt{\epsilon}2^4\,|\,L_{\perp}^{\mathrm{out}}(\omega_s)L_{\perp}^{\mathrm{out}}(\omega)\,|^2_{\mathrm{hemisph}}\ ,$$

with ω and ω_s being the incoming and Raman scattering frequencies, respectively.

Both the SH and Raman enhancements have essentially the same dependence on the local-field factors because $\omega\sim\omega_s$ in the Raman case, while the SH radiation is predominantly from hemispheroids resonant at the fundamental frequency ω and far off-resonant at 2ω with $L(2\omega)\sim 1$. Relating the inside and outside local-field factors using Eq. (2) allows us to conclude that both η_{SH} and η_R are proportional to $|\,L_{\perp}^{\mathrm{out}}(\omega)\,|^4$.

In the SHG experiment, if we assume that the second-order polarizabilities of the smooth and rough surfaces in our experiment were the same, due to their similar preparation conditions, we can then compare our measurements with the predictions of Eqs. (9) or (10). Since all the materials were evaporated on the same roughened slide, the rough surface morphology was identical for all of them. Then, we eliminate C in Eq. (10) by always

TABLE II. Dielectric constants.

Material	$\epsilon_m(\lambda=1.06\ \mu m)$	$\epsilon_m(\lambda=0.532\ \mu m)$
$_{31}$Ga	$-152 + i9.2$	$-37.7 + i1.17$
$_{13}$Al	$-100 + i25.7$	$-36.6 + i11.5$
$_{47}$Ag	$-58.14 + i0.610$	$-11.78 + i0.371$
$_{12}$Mg	$-85.4 + i3.66$	$-20.8 + i0.46$
$_{11}$Na	$-22.5 + i0.57$	$-4.79 + i0.24$
$_{19}$K	$-10.41 + i0.268$	$-1.92 + i0.133$
$_{37}$Rb	$-8.0 + i0.057$	$-1.22 + i0.229$
$_{82}$Pb	$-40.8 + i24.0$	$-11.3 + i20.8$
$_{28}$Ni	$-27.3 + i30.5$	$-8.72 + i13.16$
$_{50}$Sn	$-50.0 + i59$	$-55 + i16.5$
$_{29}$Cu	$-49.13 + i4.91$	$-5.50 + i5.76$
$_{83}$Bi	$-5.22 + i39.0$	$-12.2 + i12.5$
$_{79}$Au	$-48.24 + i3.59$	$-4.71 + i2.42$
$_{32}$Ge	$18.9 + i1.02$	$19.3 + i21.1$
$_{49}$In	$-58.4 + i34.9$	$-21.9 + i9.7$
$_{26}$Fe	$-7.16 + i23.6$	$-.12 + i16.9$
$_{25}$Mn	$-9.6 + i29.2$	$-5.17 + i15.37$

referring the SH enhancement to that of a chosen standard material. Therefore, the relative η_{SH}^T should be calculated to compare with the measured relative SH enhancement. To calculate $\eta_{SH}(a,b)$, we have used the dielectric constants listed in Table II, which were taken from the most recent literature values, or for Ga and Mg, calculated from the Drude model. Because of the local-plasmon-resonance function L_p, $\eta_{SH}(a,b)$ peaks at particular values of a and b for each material. It then allows us to limit the summation in Eq. (10) to $a/b=1$ to 20 and $V/\lambda^3=10^{-5}$ to 10^{-4}, for all the materials. At $\lambda=1.06\ \mu m$, this range roughly describes shapes and sizes of the protrusions seen in electron photomicrographs of the actual roughened surfaces.

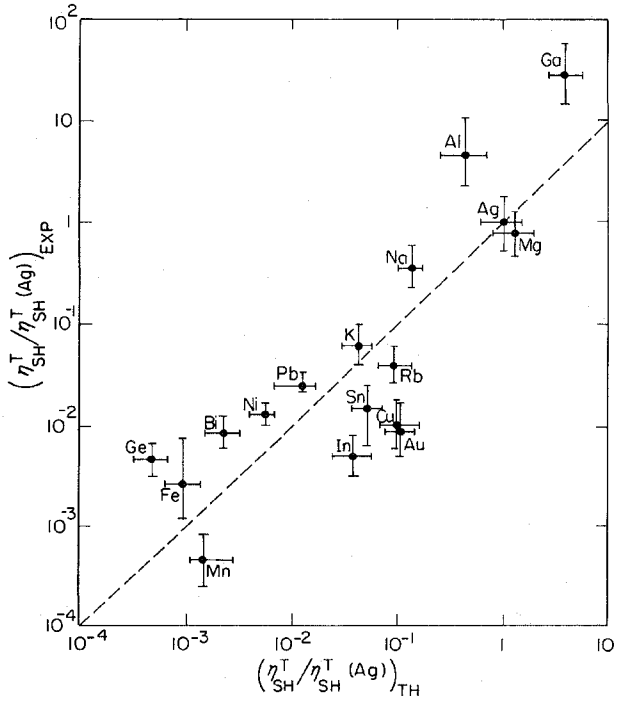

FIG. 4. Experimental versus theoretical SH enhancements, relative to silver.

The measured and calculated values of the SH enhancements relative to silver are compared in Fig. 4. For perfect agreement, the experimental data would lie on the dashed line. It is seen that overall, the local-field theory is accurate to better than an order of magnitude, for measurements which ranged over 4 orders of magnitude. The experimental error bars indicate the reproducibility of each measurement. The theoretical error bars were derived either from the published accuracy of the dielectric constants or the parameters needed to calculate them.

The fractional coverage factor C in Eq. (10) may be deduced from the ratio of the measured η_{SH}^T to the calculated summations of $\eta_{SH}(a,b)$. For all of the materials it was found that $C\simeq 3\times 10^{-4}$, for summations carried out at a fixed optimum V, and $\Delta(a/b)=0.1$. Thus, an average of 0.03% of the surface is occupied by protrusions with an effective a/b lying between $a/b-0.1$ and $a/b+0.1$. An examination of photomicrographs of the rough surface shows this to be a reasonable result.

IV. DISCUSSION

The success of the simple model of the rough surface is somewhat surprising, since the actual surfaces hardly resemble a distribution of isolated hemispheroids on a conducting plane. This is presumably because the model emphasizes the local-field contributions of the lightning-rod and local-plasmon-resonance effects, which occur predominantly at the tips of the surface protrusions. At a given excitation frequency, only those tips with the proper shape are resonantly excited. They are sufficiently rare to be considered as noninteracting. Even if a cluster of protrusions resonate collectively,[20] the resonance may be approximated by that of a properly shaped single hemispheroid.

The observed wide range of the SH enhancements on different materials can be understood from the local-field model. The largest enhancements came from good conductors with relatively high electron densities. In Fig. 2(b), we notice that at the same excitation frequency, the plasmon resonance should occur in more elongated protrusions for metals with higher electron densities, giving rise to a larger lightning-rod effect. This explains why Al and Ga, having calculated plasmon resonances at $a/b=13.3$ and 12.0, respectively, have a larger SH enhancement than Na, whose lower electron density shifts the resonant shape to $a/b=3.3$. The poorer conductors, such as Pb, Sn, and Ni, have still lower enhancements due to their higher intrinsic $\mathrm{Im}(\epsilon_m)$ which damps the plasmon resonance. This effect is partially offset, however, by the broader width of L_p, as a function of a/b, which means that more protrusions can contribute near resonantly to the enhancement. The enhancement on rough Ge should be due to the lightning-rod effect alone, since the positive dielectric constant of Ge precludes any plasmon resonance. A local-field model more suited to insulators and semiconductors should presumably include oblate as well as prolate hemispheroids on a dielectric plane.

The above considerations also apply to the local-field

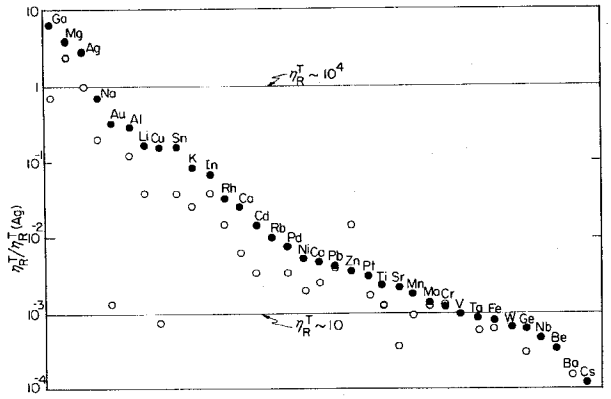

FIG. 5. Theoretical local-field Raman enhancements relative to Ag at 0.53 μm, for excitation at $\lambda=0.65$ μm (solid circles) and 0.53 μm (open circles). Points are displayed horizontally for clarity only.

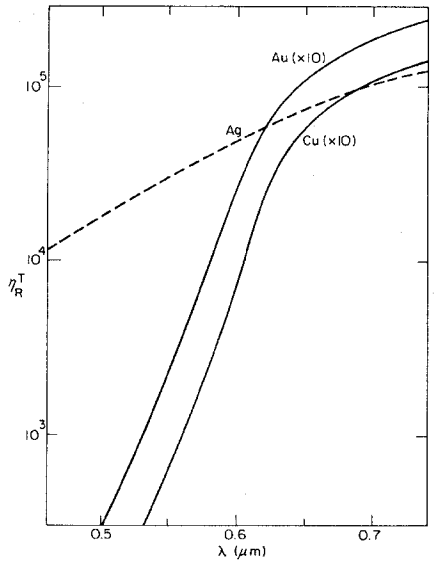

FIG. 6. Theoretical dispersion of local-field enhancements for the noble metals, for $\omega-\omega_R=1000$ cm^{-1} and $\epsilon=1$.

enhancement for Raman scattering, due to the common $|L_\perp^{\mathrm{out}}(\omega)|^4$ dependence. We have used Eqs. (10) and (11) to calculate the enhancements for various materials relative to silver. The sum in Eq. (11) is taken over the same range as in the calculation of the SH enhancement and the approximation $\epsilon_m(\omega)=\epsilon_m(\omega_R)$ is used. The ambient is chosen to be vacuum with $\epsilon=1$. Two excitation wavelengths of 0.53 and 0.65 μm are considered to illustrate the marked dispersion of some materials in the visible range of the spectrum. The results of the calculations are shown in Fig. 5. The values of η_R^T/η_R^T (Ag, 0.53 μm) are listed in decreasing order and extended horizontally for clarity only. Using $C=3\times10^{-4}$ from the SH measurements, we estimate the absolute value of η_R^T (Ag, 0.53 μm)$\simeq 2\times10^4$. From Fig. 5, it is seen that the surface local-field enhancement for surface Raman scattering can be significant for many roughened materials not yet explored in SERS studies. Several of the materials can have enhancements exceeding that of silver.

The Raman calculations appear to be reasonable. For a SERS enhancement of a factor of 10^6 for pyridine on roughened silver, η_R^T (0.53 μm)$=2\times10^4$ implies an additional enhancement of a factor of 50 due to chemical interactions. The dramatic drop in SERS for Cu and Au, when the excitation wavelength is decreased (Fig. 5), has been confirmed by many experiments.[1,28–30] The calculated dispersion of SERS is shown for the three noble metals in Fig. 6, assuming a Raman shift $\omega-\omega_R=1000$ cm^{-1}. The general trend of decreasing η_R^T with decreasing wavelength for most of the metals can be qualitatively understood from the free-electron model. The plasmon-resonance condition, $A\simeq(\omega_0/\omega_p)^3\epsilon$, tells us that decreasing the excitation wavelength increases $A(a/b)$, and shifts the resonance to less elongated protrusions. This results in a smaller lightning-rod enhancement, which diminishes η_R^T.

As a by-product of our experiment, we can estimate the second-order nonlinear optical coefficients for various materials from the SH measurements on smooth surfaces. We again take $\alpha^{(2)}_{\|\perp\|}$ as the dominant component of $\alpha^{(2)}$, neglecting contributions from possible surface contaminants. The coefficient $\alpha^{(2)}_{\|\perp\|}$ is proportional to the coefficient β often used in the literature:[31–35] $N\alpha^{(2)}_{\|\perp\|}=[\epsilon_m(\omega)-\epsilon(\omega)]\beta$, where N is the molecular density.[18] According to Eq. (7), the value of β for a given material relative to a standard material can be deduced from the ratio of the SH powers:

$$\frac{P_{\mathrm{SH}}(2\omega)}{P_{\mathrm{SH},S}(2\omega)}=\frac{|\beta|^2}{|\beta_S|^2}\frac{|\epsilon_m(\omega)-\epsilon(\omega)|^2}{|\epsilon_m(\omega)-\epsilon(\omega|_S^2}\times\frac{|L_{\|}^{\mathrm{in}}(2\omega)L_{\perp}^{\mathrm{in}}(2\omega)L_{\|}^{\mathrm{in}}(\omega)|^2_{\mathrm{plane}}}{|L_{\|}^{\mathrm{in}}(2\omega)L_{\perp}^{\mathrm{in}}(2\omega)L_{\|}^{\mathrm{in}}(\omega)|^2_{S,\mathrm{plane}}}.$$

Using the data in Table I and the dielectric constants in the literature, the ratios of β/β(Ag) can be computed and

TABLE III. Second-order optical coefficients relative to $_{47}$Ag.

Material	β/β ($_{47}$Ag)
$_{31}$Ga	0.26
$_{13}$Al	0.40
$_{12}$Mg	1.2
$_{11}$Na	1.8
$_{19}$K	2.5
$_{37}$Rb	2.2
$_{82}$Pb	0.31
$_{28}$Ni	0.14
$_{50}$Sn	0.94
$_{29}$Cu	1.2
$_{83}$Bi	0.78
$_{79}$Au	1.9
$_{32}$Ge	0.29
$_{49}$In	1.1
$_{26}$Fe	0.39
$_{25}$Mn	0.27

are listed in Table III. For most of the metals, the values of β are within a factor of 2 of one another. This tends to confirm the prediction of the free-electron model of metals that leads to $\beta = e/8\pi m^* \omega^2$,[31,32] which is independent of the free-electron density, assuming that the effective electron mass m^* is close to m. Notable exceptions to this in Table III are Ga, Pb, and Ni, in which interband contributions to β may play a significant role. A truly accurate measurement of all the nonlinear optical coefficients would require a systematic study of the intensity and phase of the SH, using a variety of input angles and polarizations, on clean surface in an ultrahigh-vacuum environment.

ACKNOWLEDGMENTS

One of us (Th.R) gratefully acknowledges support by IBM. This work was supported by the Director, Office of Energy Research, Office of Basic Energy Sciences, Materials Sciences Division of the U.S. Department of Energy under Contract No. DE-AC03-76SF00098.

---

*Permanent address: Departamento de Fisica, Universidade Federal de Pernambuco, 50000 Recife, Pernambuco, Brazil.

[1]For a recent review, see *Surface Enhanced Raman Scattering,* edited by R. K. Chang and T. E. Furtak (Plenum, New York, 1982).

[2]H. Yamada and T. Yamamoto, Chem. Phys. Lett. **77**, 520 (1981).

[3]H. Yamada, Y. Yamamoto, and N. Tani, Chem. Phys. Lett. **86**, 397 (1982).

[4]R. P. Cooney, E. S. Reid, P. J. Hendra, and M. Fleishmann, J. Am. Chem. Soc. **99**, 2002 (1977).

[5]W. Krasser and A. J. Renouprez, Solid State Commun. **41**, 231 (1982).

[6]V. V. Masinyuk, R. M. Lazorenko-Manevich, and Ya. M. Kolotyrkin, Solid State Commun. **43**, 721 (1982).

[7]B. H. Loo, Solid State Commun. **43**, 349 (1982).

[8]T. E. Furtak and J. Kester, Phys. Rev. Lett. **45**, 1652 (1980).

[9]M. Fleischmann, P. R. Graves, I. R. Hill, and J. Robinson, Chem. Phys. Lett. **95**, 322 (1983).

[10]W. Krasser, in *Proceedings of the VIIth International Conference on Raman Spectroscopy, Ottawa, 1980,* edited by W. F. Murphy (North-Holland, Amsterdam, 1980), p. 420.

[11]L. A. Sanchez, R. L. Birke, and J. R. Lombardi, Chem. Phys. Lett. **79**, 219 (1981).

[12]R. Naaman, S. J. Beulow, O. Cheshnovsky, and D. R. Herschbach, J. Phys. Chem **84**, 2692 (1980).

[13]P. A. Lund, R. R. Smardzewskii, and D. E. Tevault, Chem. Phys. Lett. **89**, 508 (1982).

[14]B. H. Loo, J. Chem. Phys. **75**, 5955 (1981).

[15]P. F. Liao and M. B. Stern, Opt. Lett. **7**, 483 (1982).

[16]J. E. Potts, R. Merlin, and D. L. Partin, Phys. Rev. B **27**, 3905 (1983).

[17]J. C. Tsang and J. Kirtley, Solid State Commun. **30**, 617 (1979).

[18]C. K. Chen, T. F. Heinz, D. Ricard, and Y. R. Shen, Phys. Rev. B **27**, 1965 (1983), and references therein.

[19]C. K. Chen, A. R. B. de Castro, and Y. R. Shen, Phys. Rev. Lett. **46**, 145 (1981).

[20]U. Laor and G. C. Schatz, Chem. Phys. Lett. **82**, 566 (1981); J. Chem. Phys. **76**, 2888 (1982).

[21]P. C. Das and J. I. Gersten, Phys. Rev. B **25**, 6281 (1982).

[22]P. Ye and Y. R. Shen, Phys. Rev. B **28**, 4288 (1983).

[23]J. Gersten and A. Nitzan, J. Chem. Phys. **73**, 3023 (1980); **75**, 1139 (1981).

[24]P. F. Liao and A. Wokaun, J. Chem. Phys. **76**, 751 (1982).

[25]J. A. Stratton, *Electromagnetic Theory* (McGraw-Hill, New York, 1941), Chap. 3.

[26]For explicit tabulation of A, see J. A. Osborn, Phys. Rev. **67**, 351 (1945); E. C. Stoner, Philos. Mag. **36**, 803 (1945).

[27]A. Wokaun, J. P. Gordon, and P. F. Liao, Phys. Rev. Lett. **48**, 957 (1982).

[28]R. K. Chang, in *Lasers and Applications, Proceedings of the Sergio Porto Memorial Symposium, Brazil,* 1980, edited by W. O. N. Guimaraes, C.-P. Lin, and A. Mooradian (Springer, Berlin, 1980), p. 55.

[29]T. E. Furtak, in *Proceedings of the VIIth International Conference on Raman Spectroscopy,* Ottawa, 1980, edited by W. F. Murphy (North-Holland, Amsterdam, 1980), p. 380; B. Pettinger, *ibid.*, p. 412.

[30]C. S. Allen, G. C. Schats, and R. P. Van Duyne, Chem. Phys. Lett. **75**, 201 (1980).

[31]N. Bloembergen, R. K. Chang, S. S. Jha, and C. H. Lee, Phys. Rev. **174**, 813 (1968); **178**, 1528(E) (1969).

[32]J. Rudnick and E. A. Stern, Phys. Rev. B **4**, 4274 (1971).

[33]C. S. Wang, J. M. Chen, and J. R. Bower, Optics Commun. **8**, 275 (1973).

[34]J. R. Bower, Phys. Rev. B **14**, 2427 (1976).

[35]J. E. Sipe, V. C. Y. So, M. Fukui, and G. I. Stegeman, Phys. Rev. B **21**, 4389 (1980).